

Support Information

Theoretical probing possible degradation mechanisms of FeNC catalyst during oxygen reduction reaction

Na Yang,^{a, b, c} Lanlan Peng,^a Li Li,^{*, a} Jing Li,^a Qiang Liao,^d Minghua Shao,^e and Zidong

Wei^{*, a}

^a The State Key Laboratory of Power Transmission Equipment & System Security and New Technology, Chongqing Key Laboratory of Chemical Process for Clean Energy and Resource Utilization, School of Chemistry and Chemical Engineering, Chongqing University Shazhengjie 174, Chongqing 400044(China)

^b Department of Chemical Engineering, Waterloo Institute for Nanotechnology, Waterloo Institute for Sustainable Energy, University of Waterloo, Waterloo, ON, N2L 3G1(Canada)

^c School of Information and Optoelectronic Science and Engineering, South China Normal University, Guangzhou, 510006(China)

^d The Key Laboratory of Low-Grade Energy Utilization Technologies and Systems, Chongqing, 400044(China)

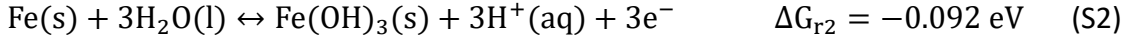
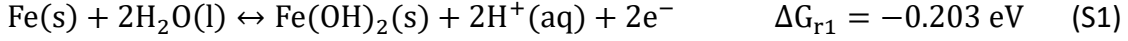
^e Department of Chemical and Biomolecular Engineering, The Hong Kong University of Science and Technology, Clear Water Bay, Kowloon, Hong Kong

*Corresponding author's

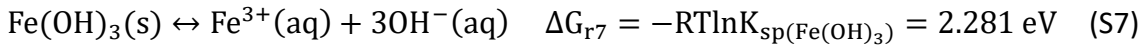
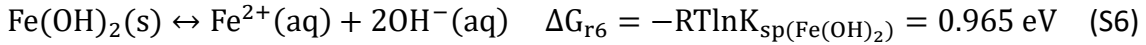
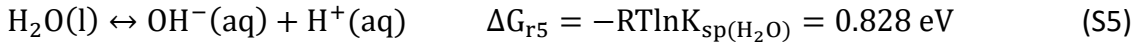
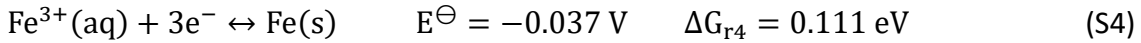
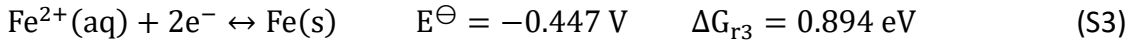
E-mail: liliracial@cqu.edu.cn (Li); zdwei@cqu.edu.cn (Wei), Tel: +86 2365678945

The thermodynamic calculation of FeOR mechanism during ORR process

Generally, in an acid electrolyte ($[H^+] = 1 \text{ mol/L}$, $\text{pH}=0$), H_2O can act as the OH^- donor, the oxidation of Fe site on FeNC catalyst, and formed of $\text{Fe}(\text{OH})_2(\text{s})$ or $\text{Fe}(\text{OH})_3(\text{s})$ can be written as:

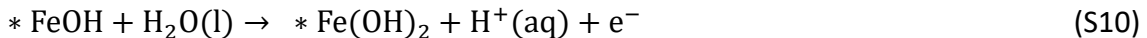
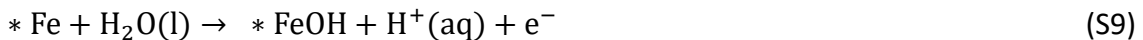


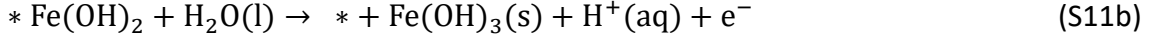
Here, the reaction free energy ($\Delta G_{r1} = 2\Delta G_{r5} - \Delta G_{r3} - \Delta G_{r6}$ and $\Delta G_{r2} = 3\Delta G_{r5} - \Delta G_{r4} - \Delta G_{r7}$) of equations (S1 and 2) are calculated using the follow equations (S3-7)^{S1}.



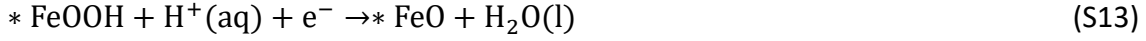
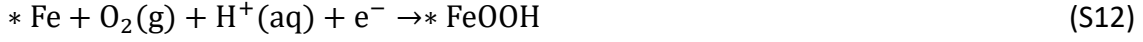
Here, the standard reduction potentials (E^\ominus values) and solubility product constant ($K_{\text{sp}(\text{H}_2\text{O})} = 4.87 \times 10^{-14}$, $K_{\text{sp}(\text{Fe}(\text{OH})_2)} = 4.87 \times 10^{-17}$ and $K_{\text{sp}(\text{Fe}(\text{OH})_3)} = 2.79 \times 10^{-39}$) at 298.15 K.

Then, the FeOR without the participation of ORR intermediates on FeNC catalyst may proceed through the following elementary steps:





While, the FeOR intermediate (i.e. *FeOH) also formation during ORR process:



where * stands for carbon-base catalyst surface without Fe site, and the (l), (aq), (g) and (s) refer to liquid, aqueous, gas and solid phase.

In this model, we set up RHE as the reference electrode, which allows us to replace chemical potential (μ) of the proton-electron pair with that of half a hydrogen molecule:

$$\mu(\text{H}^+(\text{aq}) + \text{e}^-) = \frac{1}{2} \mu_{\text{H}_2} - eU, \text{ at conditions with } P_{\text{H}_2} = 1 \text{ bar.}$$

The chemical potential of each adsorbate is defined as: $\mu = E + E_{\text{ZPE}} - TS$. where the E is the total energy obtained from DFT calculations, E_{ZPE} is the zero point energy, and S is the entropy at 298.15 K.⁵² In order to obtain the reaction free energy of each elementary step of ORR and FeOR, we calculated the adsorption free energy of *Fe, *FeO, *FeOOH, *FeOH, and *Fe(OH)₂. Because it is difficult to obtain the exact free energy of Fe, FeO, FeOOH, FeOH, Fe(OH)₂ and Fe(OH)₃ radicals in the electrolyte solution, the free energy $\Delta G_{* \text{Fe}}$, $\Delta G_{* \text{FeO}}$, $\Delta G_{* \text{FeOOH}}$, $\Delta G_{* \text{FeOH}}$, $\Delta G_{* \text{Fe}(\text{OH})_2}$, G_{O_2} , $G_{\text{Fe}(\text{OH})_2}$ and $G_{\text{Fe}(\text{OH})_3}$, are relative to the free energy of stoichiometrically appropriate amounts of $\text{H}_2\text{O}(\text{g})$ (on DFT scale, the potential of water in the gas phase is described as $\mu_{\text{H}_2\text{O}(\text{g})} = \mu_{\text{H}_2\text{O}(\text{l})}$ (T=298.15 K, P=0.035 bar), $\text{H}_2(\text{g})$, and Fe in its ground-state body-centered cubic (BCC) crystal phase, defined as follows^{52, 3}:

$$\Delta G_{* \text{Fe}} = \Delta G(\text{Fe}(\text{s}) + * \rightarrow * \text{Fe}) = \mu_{* \text{Fe}} - \mu_* - \mu_{\text{Fe}}$$

$$\begin{aligned} \Delta G_{* \text{FeOH}} &= \Delta G \left(\text{Fe}(\text{s}) + \text{H}_2\text{O}(\text{g}) + * \rightarrow * \text{FeOH} + \frac{1}{2} \text{H}_2(\text{g}) \right) \\ &= \mu_{* \text{Fe}(\text{OH})} + \frac{1}{2} \mu_{\text{H}_2} - \mu_* - \mu_{\text{Fe}} - \mu_{\text{H}_2\text{O}} \end{aligned}$$

$$\Delta G_{*Fe(OH)_2} = \Delta G(Fe(s) + 2H_2O(g) + * \rightarrow * Fe(OH)_2 + H_2(g))$$

$$= \mu_{*Fe(OH)_2} + \mu_{H_2} - \mu_* - \mu_{Fe} - 2\mu_{H_2O}$$

$$\Delta G_{*FeOOH} = \Delta G(Fe(s) + 2H_2O(g) + * \rightarrow * FeOOH + \frac{3}{2} H_2(g))$$

$$= \mu_{*FeOOH} + \frac{3}{2} \mu_{H_2} - \mu_* - \mu_{Fe} - 2\mu_{H_2O}$$

$$\Delta G_{*FeO} = \Delta G(Fe(s) + H_2O(g) + * \rightarrow * FeO + H_2(g)) = \mu_{*FeO} + \mu_{H_2} - \mu_* - \mu_{Fe} - \mu_{H_2O}$$

$$G_{Fe(OH)_2} = 2G_{H_2O(l)} - G_{H_2(g)} + G_{Fe} - 0.203 \text{ eV}$$

$$G_{Fe(OH)_3} = 3 \left(G_{H_2O(l)} - \frac{1}{2} G_{H_2(g)} \right) + G_{Fe} - 0.092 \text{ eV}$$

$$G_{O_2(g)} = 2G_{H_2O(l)} - 2G_{H_2(g)} + 4.92 \text{ eV}$$

Furthermore, for each elementary step, the reaction free energy change (ΔG_r) is defined as the difference between of free energy of the reactants and products ^{S2}:

$$\Delta G_r = \Delta E + \Delta E_{ZPE} - T\Delta S + \Delta G_U + \Delta G_{pH}$$

Then, the reaction free energy of step (S8-11a/b) can be calculated using the following equations (S16-19a/b):

$$\Delta G_{r8} = \Delta G_{*Fe} \tag{S16}$$

$$\Delta G_{r9} = \Delta G_{*FeOH} - \Delta G_{*Fe} + \Delta G_{pH}(H^+) - eU \tag{S17}$$

$$\Delta G_{r10} = \Delta G_{*Fe(OH)_2} - \Delta G_{*FeOH} + \Delta G_{pH}(H^+) - eU \tag{S18}$$

$$\Delta G_{r11a} = -0.203 \text{ eV} - \Delta G_{*Fe(OH)_2} \tag{S19a}$$

$$\Delta G_{r11b} = -0.092 \text{ eV} - \Delta G_{*Fe(OH)_2} + \Delta G_{pH}(H^+) - eU \tag{S19b}$$

And, the reaction free energy of step (S12-15) can be calculated using the following equations (S20-23):

$$\Delta G_{r12} = \Delta G_{*FeOOH} - 4.92 \text{ eV} - \Delta G_{*Fe} - \Delta G_{pH}(H^+) + eU \tag{S20}$$

$$\Delta G_{r13} = \Delta G_{*FeO} - \Delta G_{*FeOOH} - \Delta G_{pH}(H^+) + eU \tag{S21}$$

$$\Delta G_{r14} = \Delta G_{*FeOH} - \Delta G_{*FeO} - \Delta G_{pH}(H^+) + eU \quad (S22)$$

$$\Delta G_{r15} = \Delta G_{*Fe} - \Delta G_{*FeOH} - \Delta G_{pH}(H^+) + eU \quad (S23)$$

Here, $\Delta G_U = -eU$, the e is the elementary charge and U is the potential difference between electrode and RHE, here, $U^{RHE} = 0.9$ V (about the half-wave potential of FeNC catalyst when catalyzing ORR). In an acid electrolyte ($pH=0$), the free energy change of H^+ is derived according to $\Delta G_{pH}(H^+) = -k_B T \ln(10) \times pH = 0$ (k_B is Boltzmann's constant)². And when the OH desorption and the further OH adsorption of $*FeOH$ have the same probability, meaning that $\Delta G_{r10} = \Delta G_{r15}$, $U_{TMOR}^{RHE} = \frac{\Delta G_{*Fe(OH)_2} - \Delta G_{*Fe} + 2\Delta G_{pH}(H^+)}{2e}$.

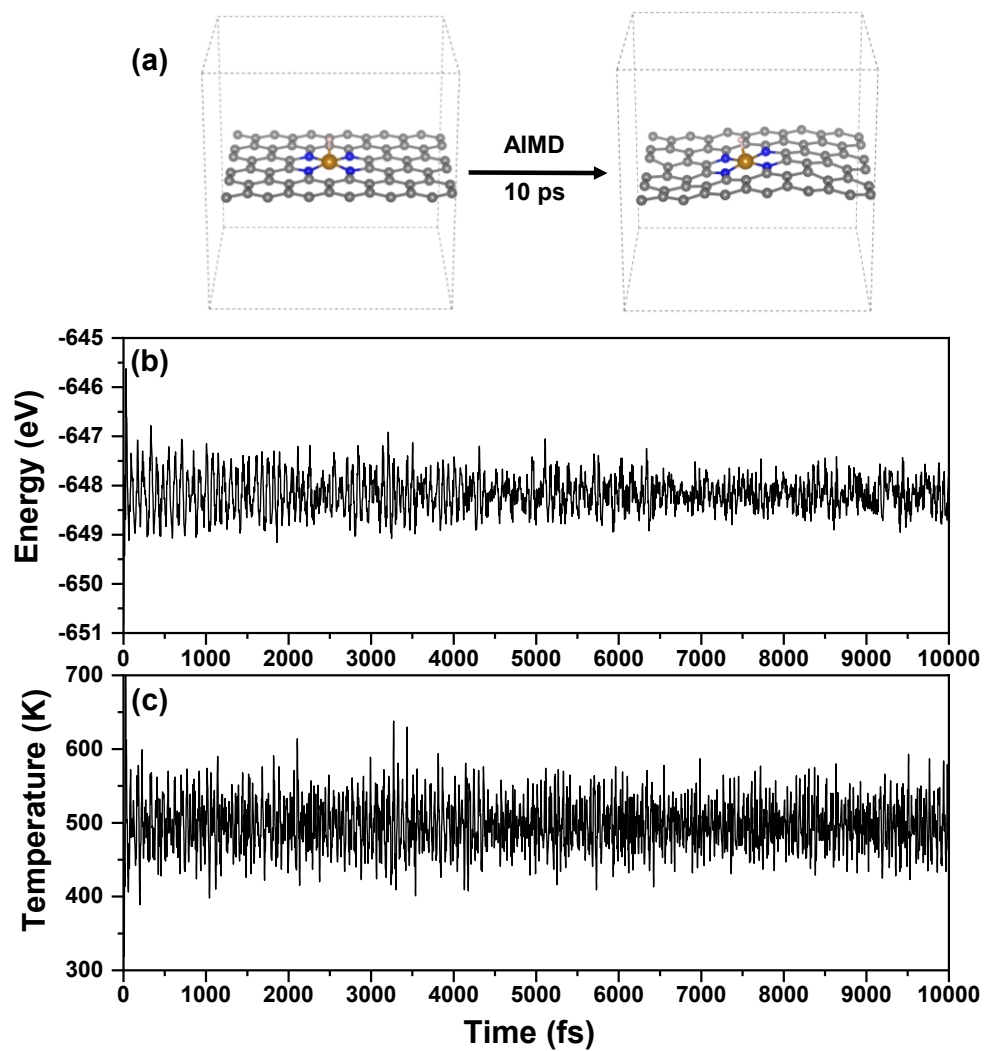


Figure S1. (a) Dynamic optimized configuration snapshot (b) total energy and (c) temperature of FeN₄H system at 500 K within 10 ps AIMD simulation.

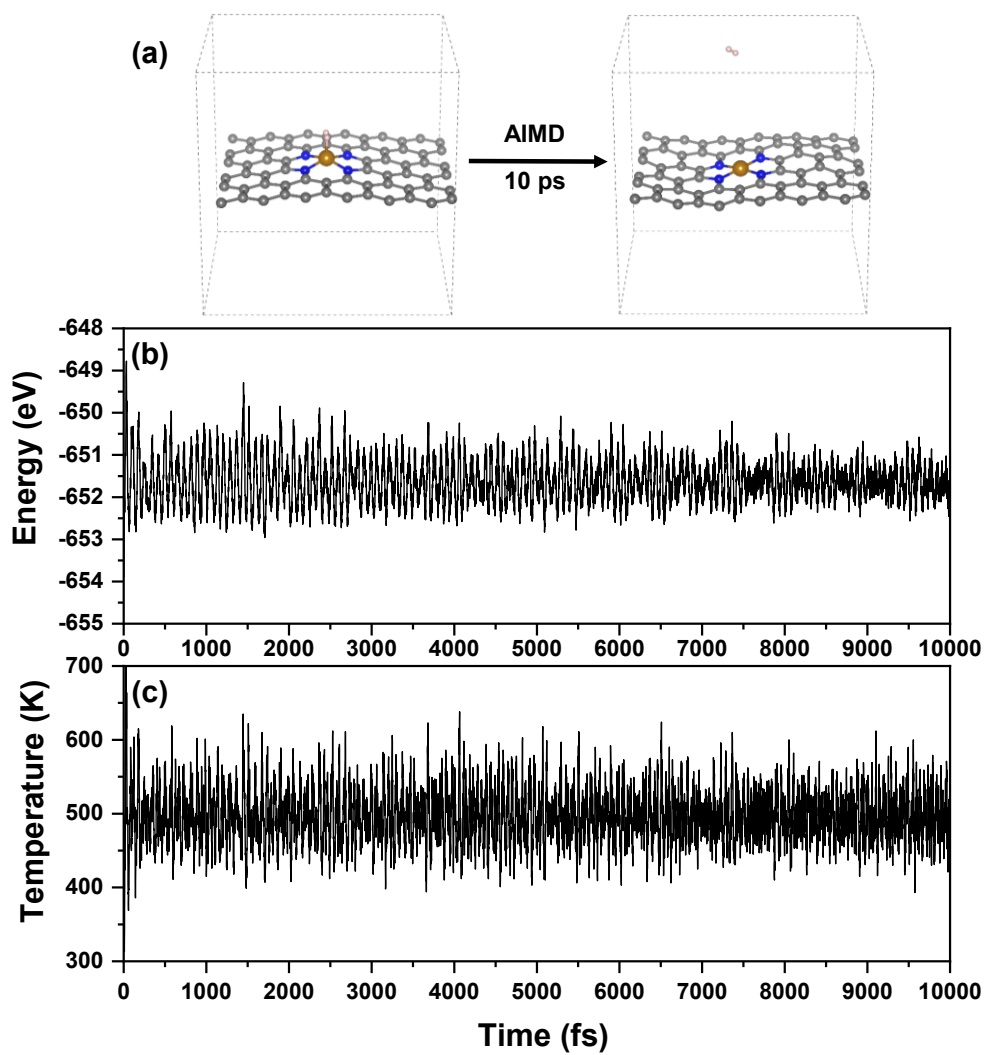


Figure S2. (a) Dynamic optimized configuration snapshot (b) total energy and (c) temperature of FeN₄H₂ system at 500 K within 10 ps AIMD simulation.

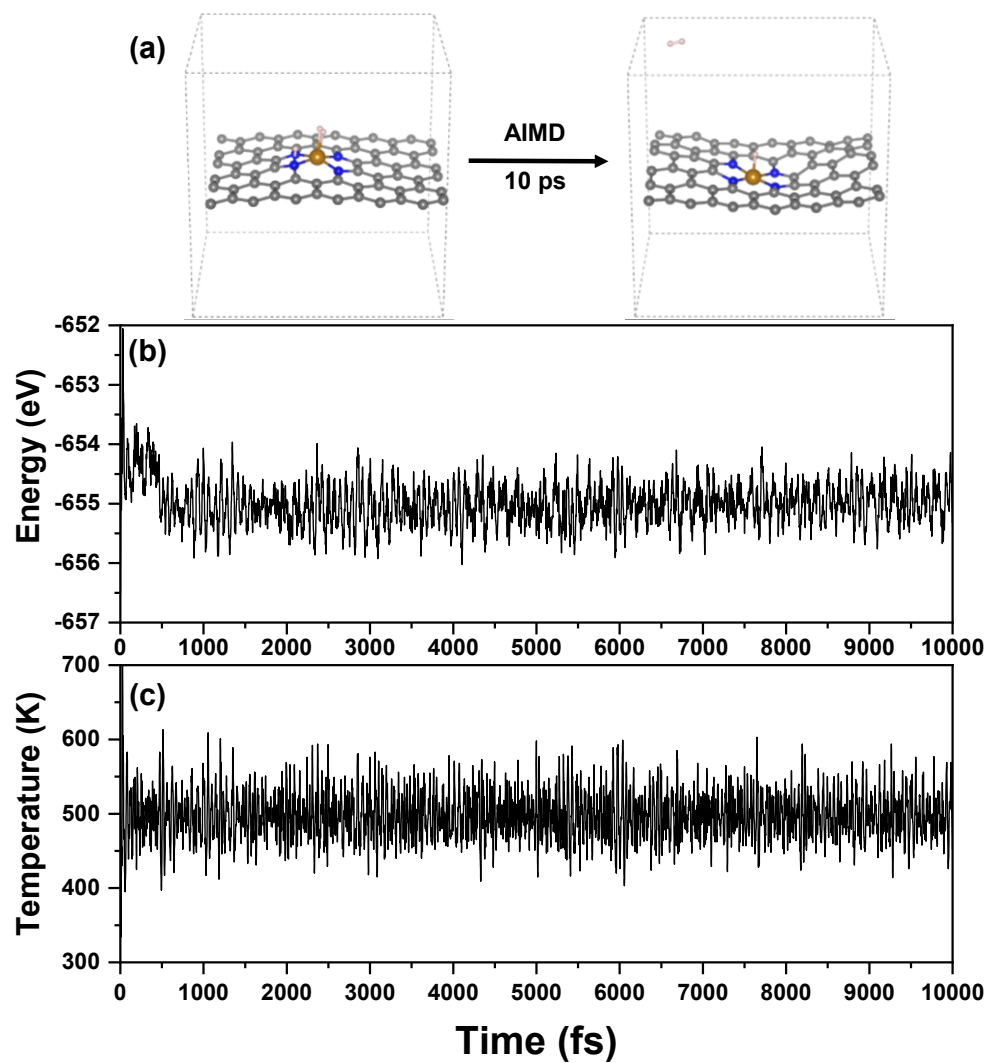


Figure S3. (a) Dynamic optimized configuration snapshot (b) total energy and (c) temperature of FeN₄H₃ system at 500 K within 10 ps AIMD simulation.

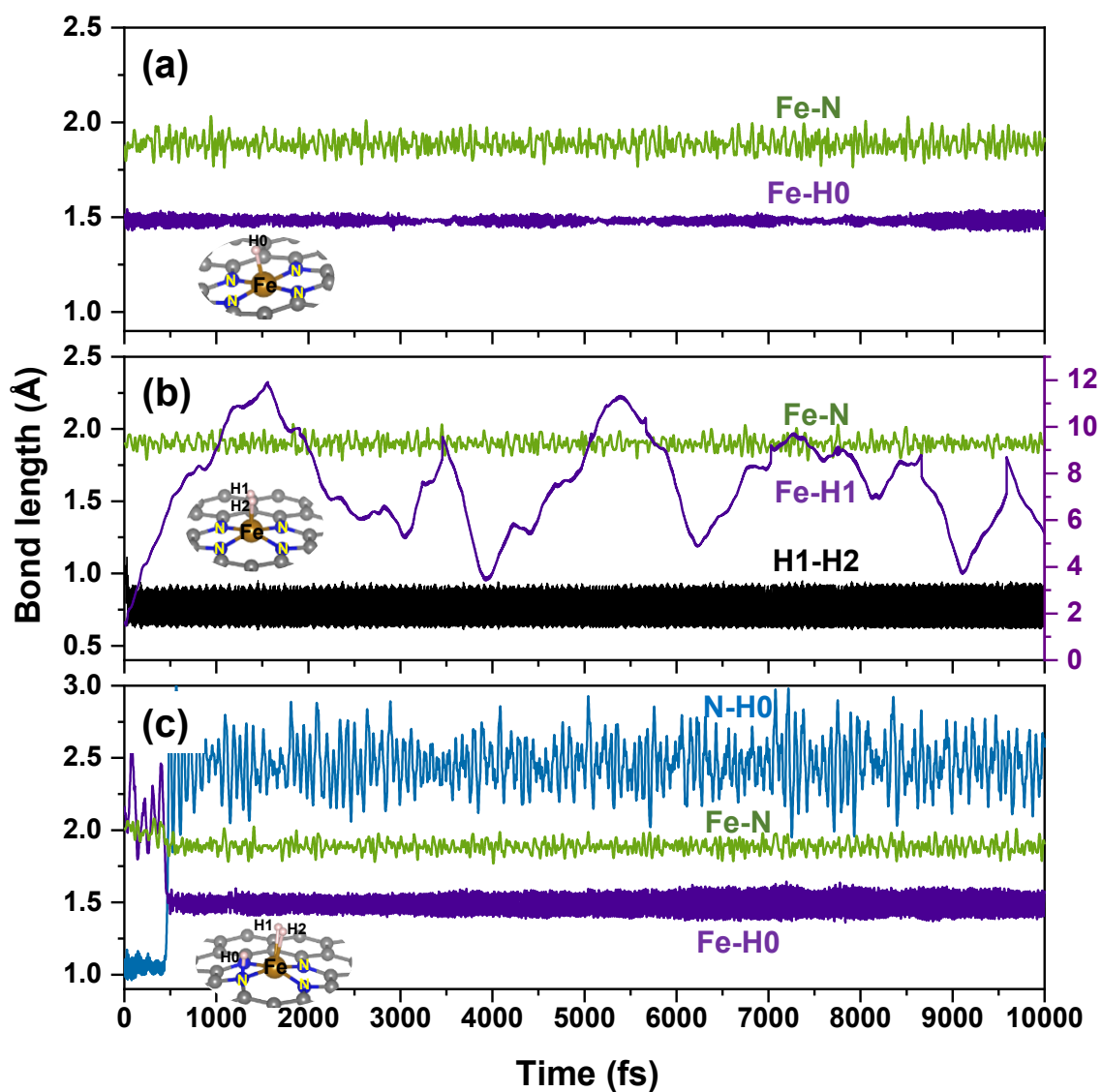


Figure S4. At 500 K within 10 ps AIMD simulation, the trajectory of different atoms pair in (a) FeN₄H, (b) FeN₄H₂ and (c) FeN₄H₃ systems.

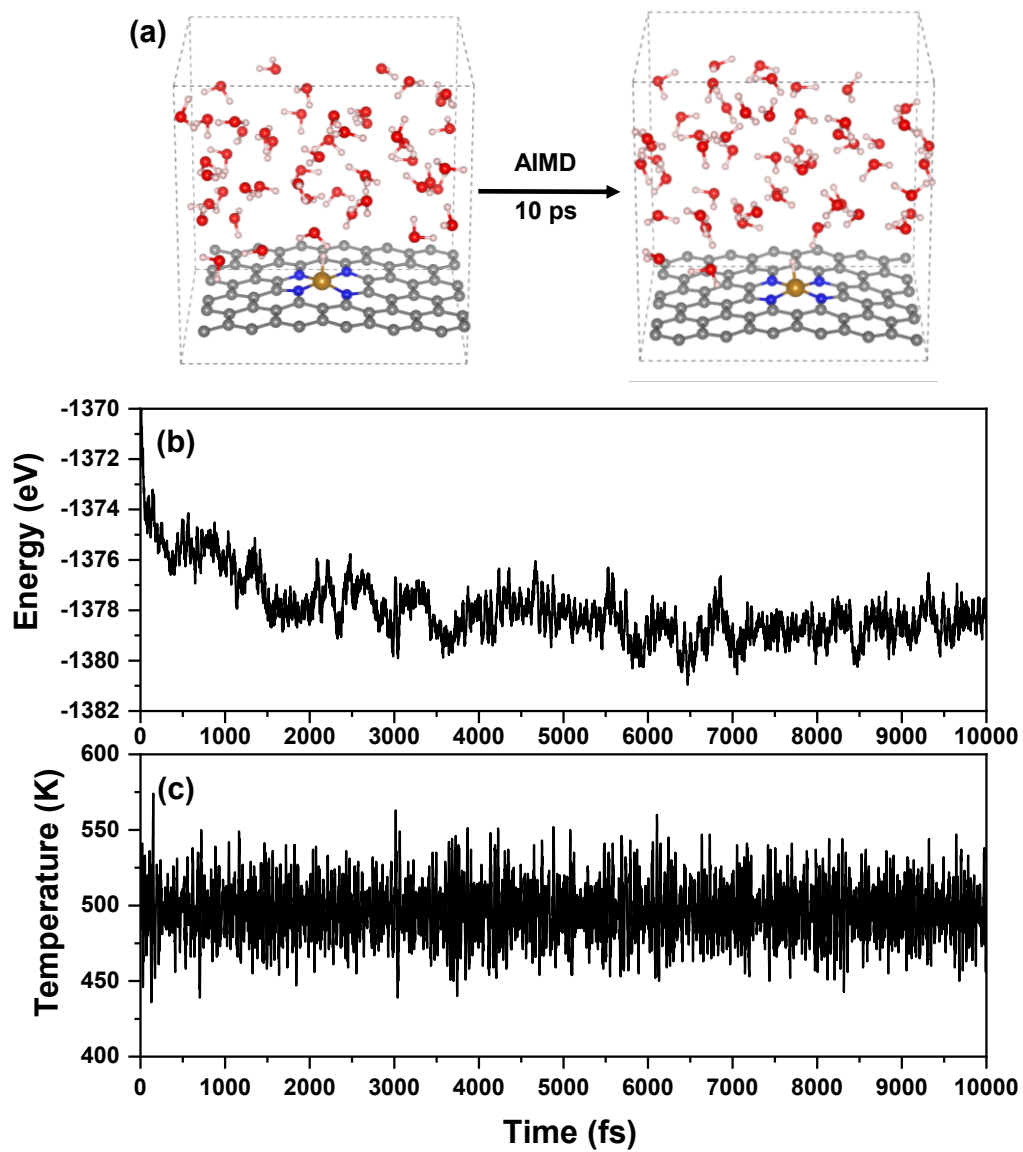


Figure S5. (a) Dynamic optimized configuration snapshot (b) total energy and (c) temperature of FeN₄H system in real water solution at 500 K within 10 ps AIMD simulation.

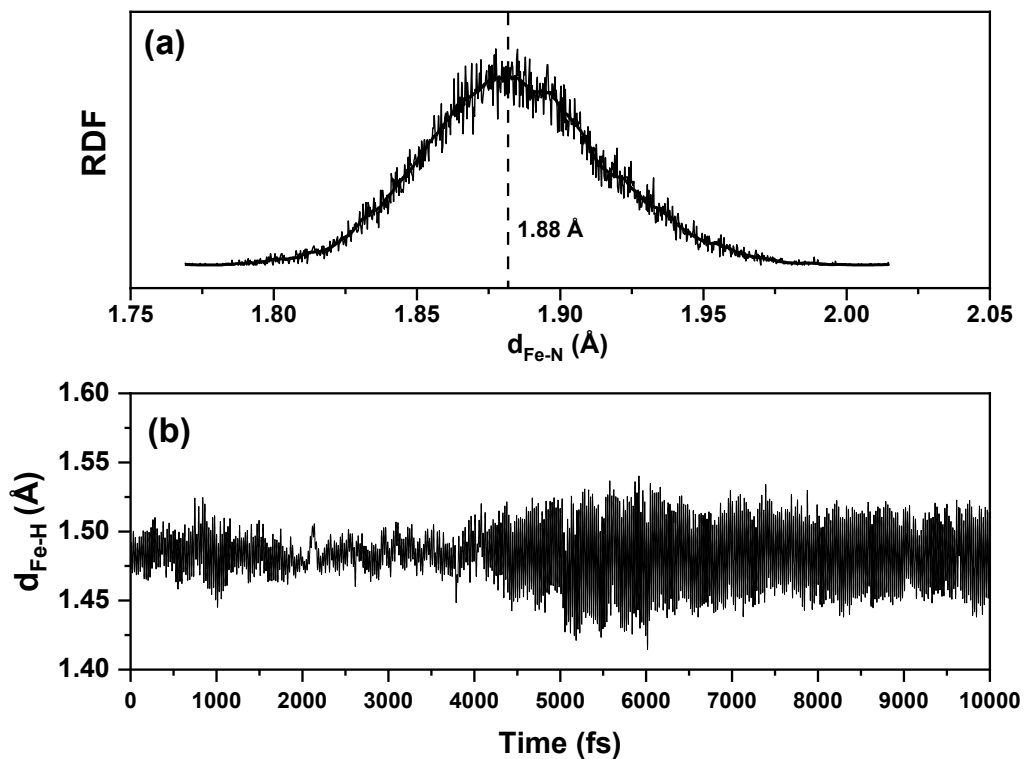


Figure S6. In real water solution at 500 K within 10 ps AIMD simulation: (a) the radial distribution functions (RDF) for Fe-N atom pair in FeN_4H system, (b) the trajectory of Fe-H atom pair in FeN_4H system.

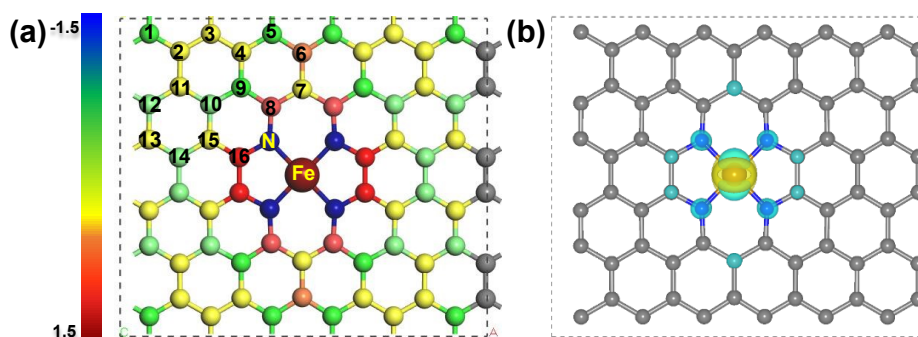


Figure S7. The charge effect (a) and spin effect (b) of FeNC surface. For the charge distribution, the color of the balls represents the value of the Bader charge, which increases gradually from blue to red. For the spin density distribution, yellow and blue iso-surfaces correspond to positive and negative spin density, respectively, and the iso-surface levels are $0.0005 \text{ e}/\text{Å}^3$.

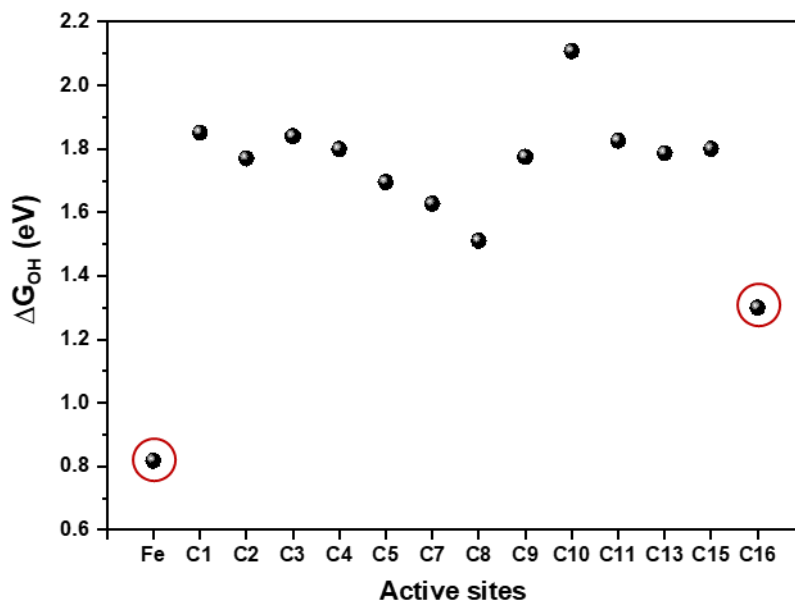


Figure S8. The free energy change value of OH adsorption (ΔG_{OH}) on Fe and 16 C sites of FeNC catalyst.

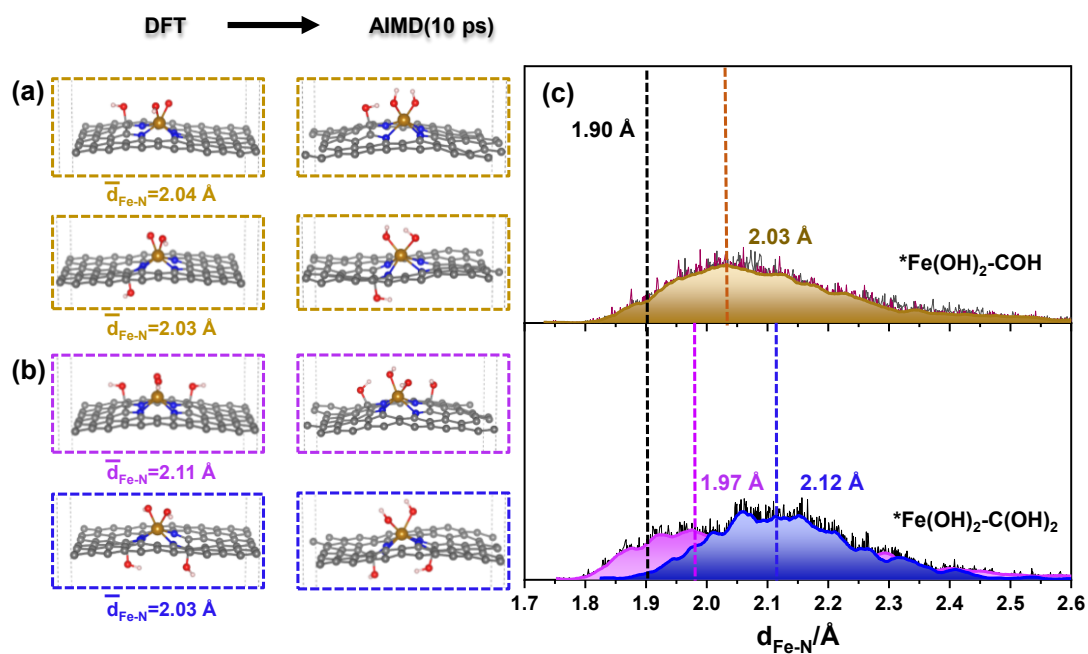


Figure S9. DFT and AIMD optimized configurations of a, b) $*Fe(OH)_2$ with COR ($*Fe(OH)_2-C(OH)_x$ ($X=1$ and 2)); c) The radial distribution functions (RDF) for Fe-N atom pairs in the $*Fe(OH)_2-C(OH)_x$ systems obtained from AIMD simulations at 500 K.

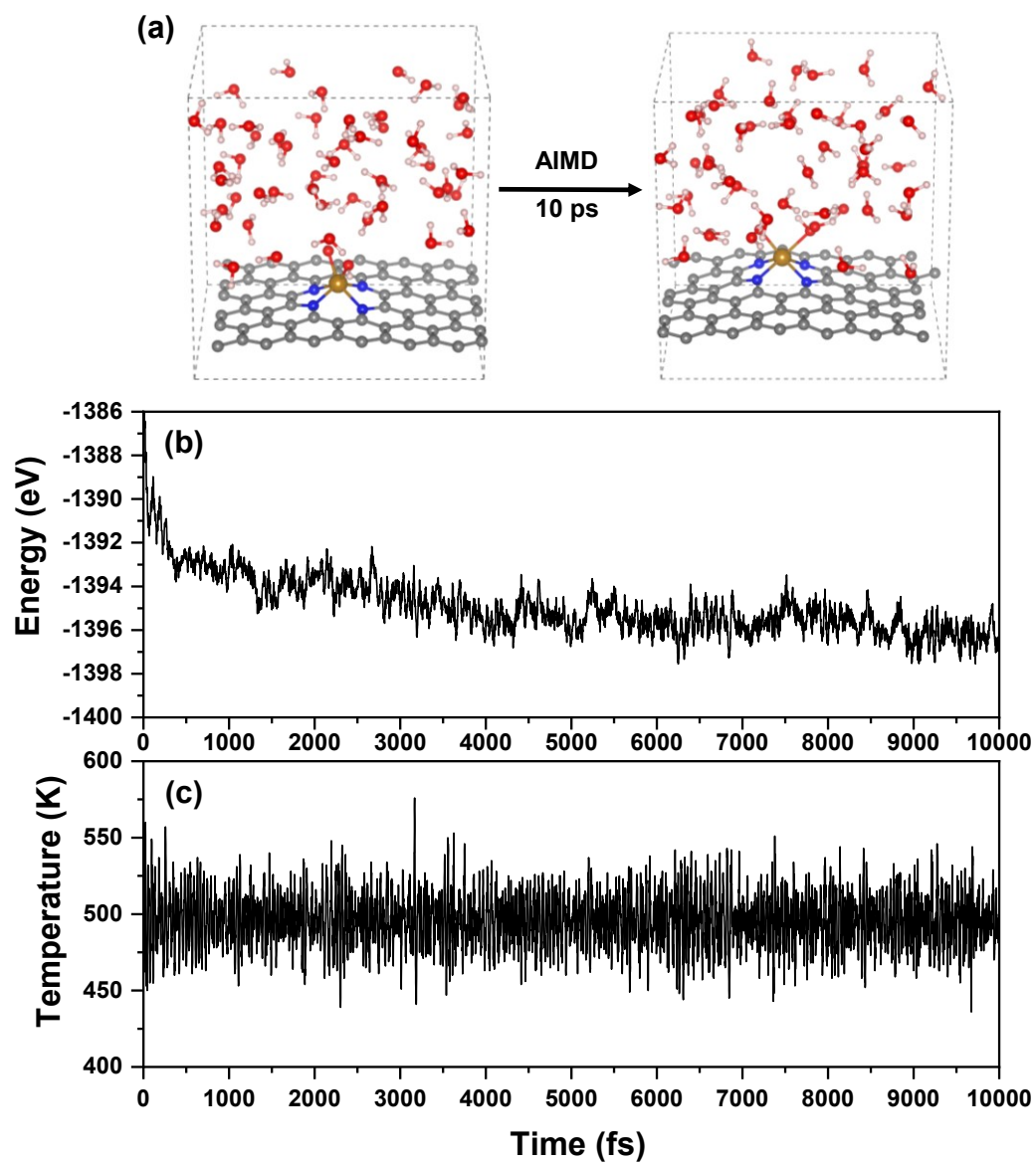


Figure S10. (a) Dynamic optimized configuration snapshot (b) total energy and (c) temperature of $^*Fe(OH)_2$ system in real water solution at 500 K within 10 ps AIMD simulation.

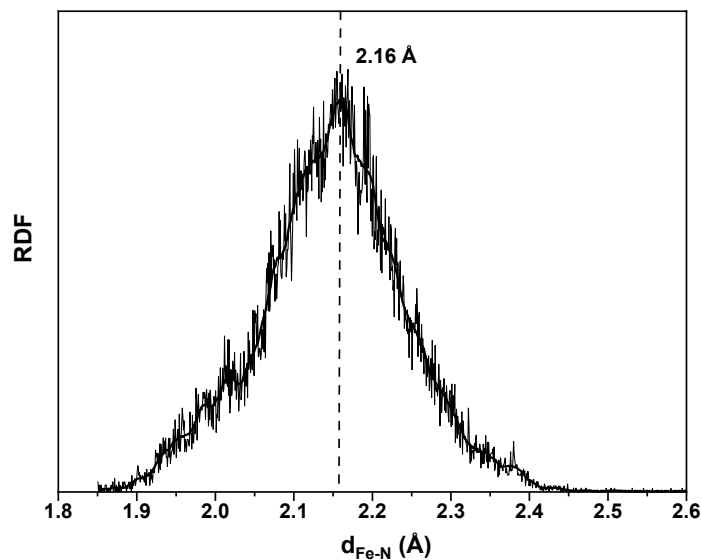


Figure S11. In real water solution at 500 K within 10 ps AIMD simulation, the radial distribution functions (RDF) for Fe-N atom pairs in $^*\text{Fe}(\text{OH})_2$ system.

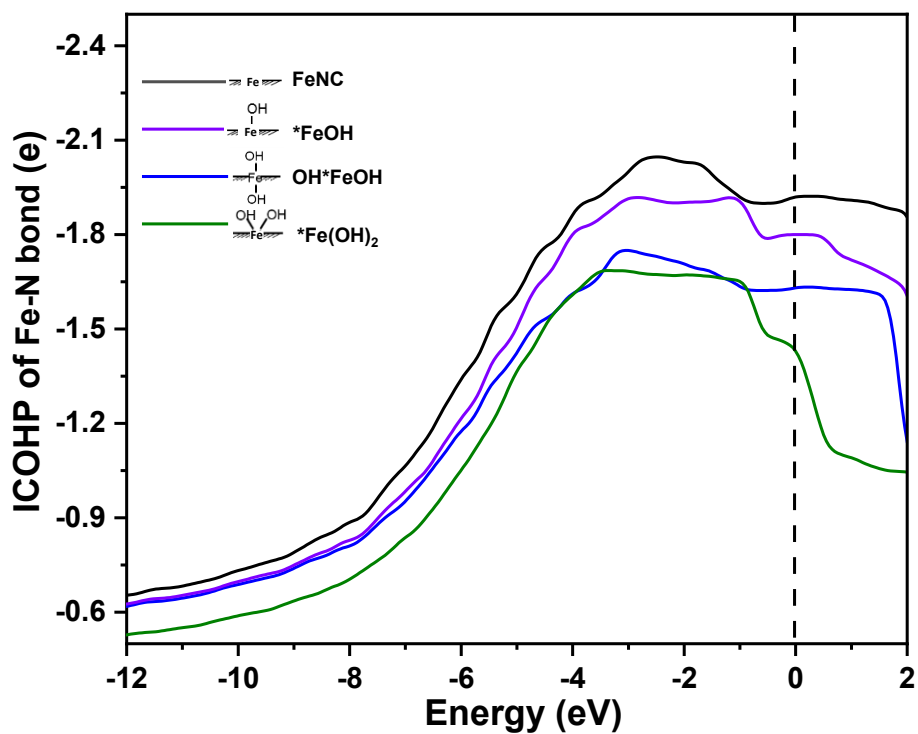


Figure S12. The average ICOHP of the Fe-N bond of clean FeNC, $^*\text{FeOH}$, OH^*FeOH and $^*\text{Fe}(\text{OH})_2$ systems.

Table S1. The Bader charge (Q), d electron number (d) on Fe atom, and the average ICOHP value of Fe-N bond.

	$Q_{Fe} (e)$	$Q_N (e)$	$d (e)$	ICOHP (e)
*FeOH	1.23	-1.17	6.18	-1.85
OH*FeOH	1.36	-1.14	6.17	-1.72
*Fe(OH) ₂	1.37	-1.18	6.15	-1.44

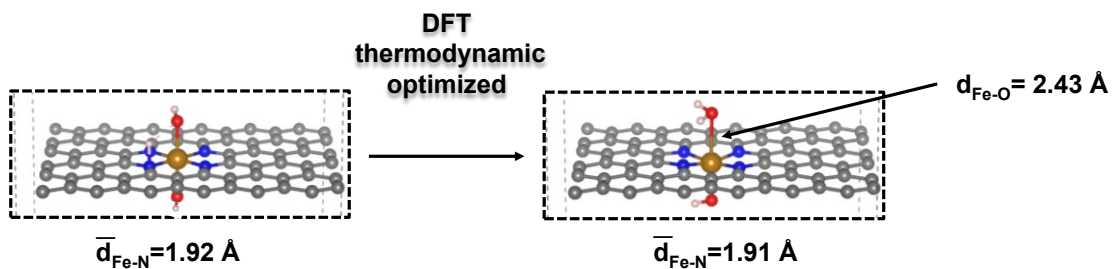


Figure S13. DFT thermodynamic optimized configuration of the OH*FeOH protonation (OH*FeOH-NH).

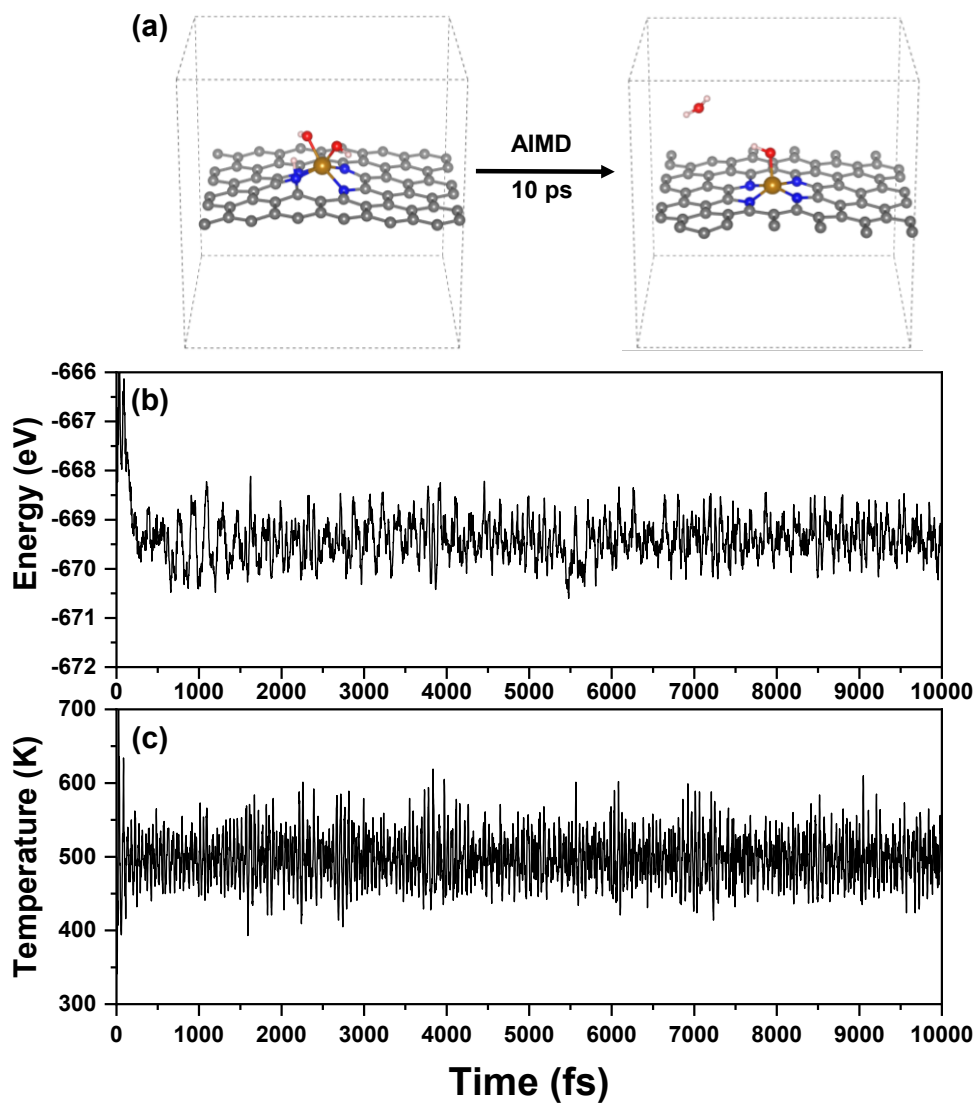


Figure S14. (a) Dynamic optimized configuration snapshot, (b) total energy and (c) temperature of $*\text{Fe}(\text{OH})_2\text{-NH}$ (proton attacks N from the same side of adsorbed OH) system at 500 K within 10 ps AIMD simulation.

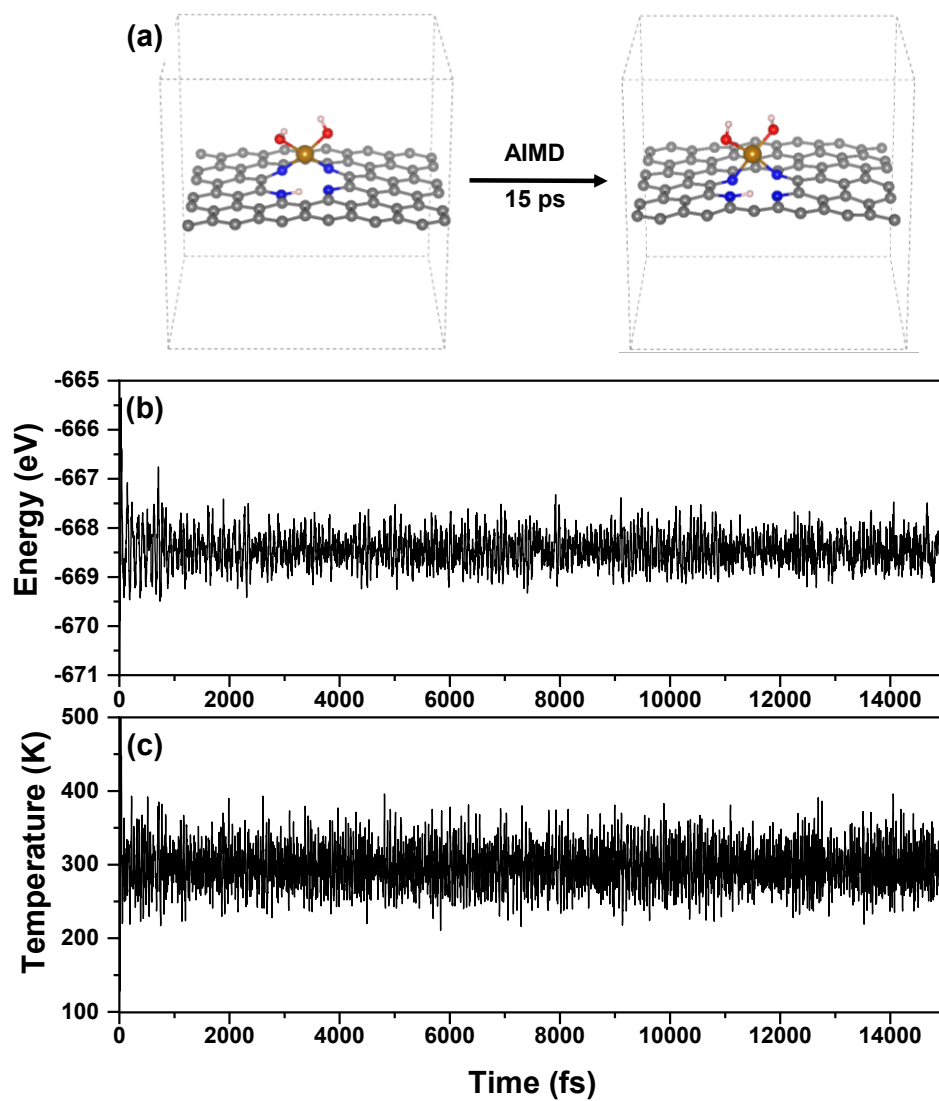


Figure S15. (a) Dynamic optimized configuration snapshot (b) total energy and (c) temperature of $*\text{Fe}(\text{OH})_2\text{-NH}$ (proton attacks N from the opposite side of adsorbed OH) system at 300 K within 15 ps AIMD simulation.

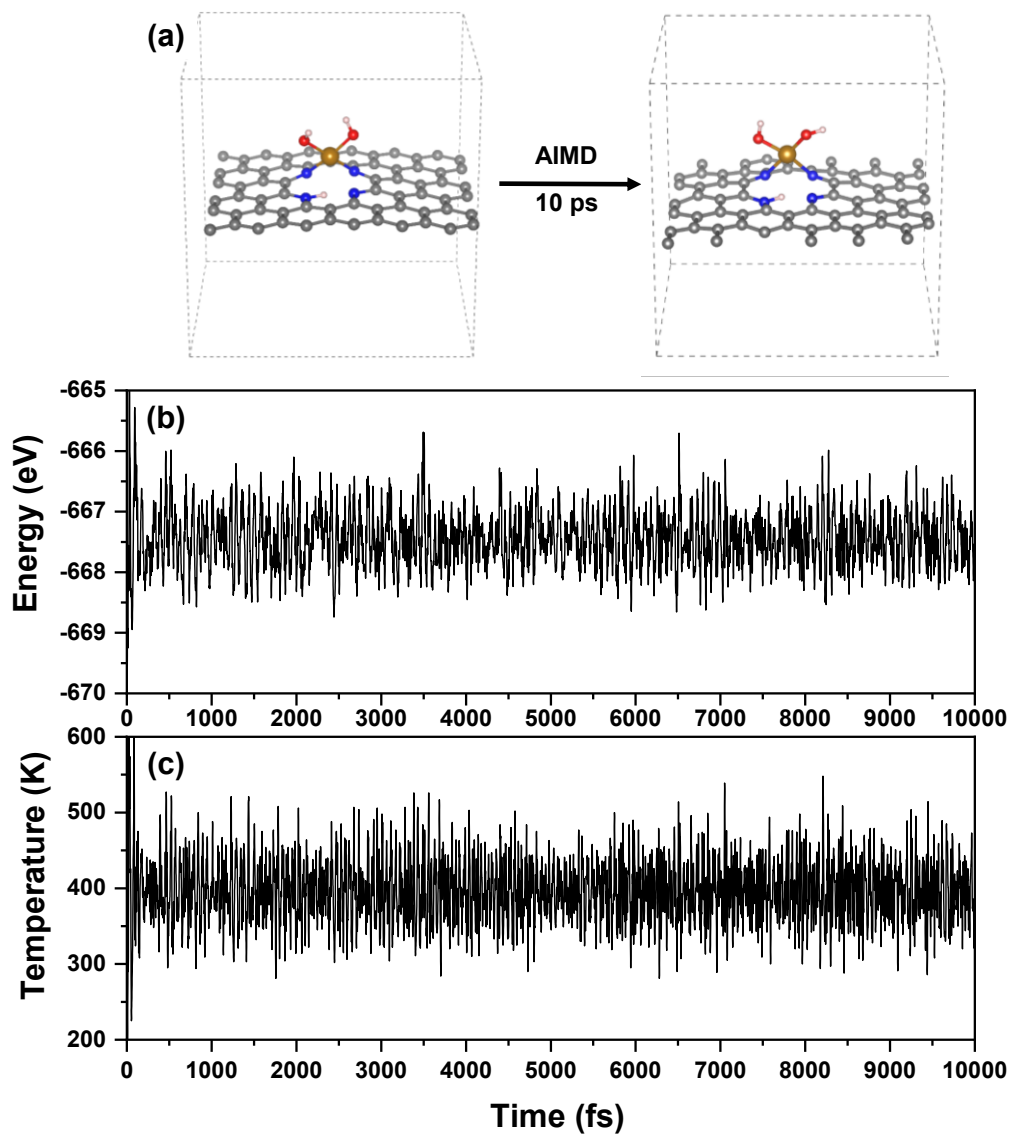


Figure S16. (a) Dynamic optimized configuration snapshot (b) total energy and (c) temperature of $*\text{Fe}(\text{OH})_2\text{-NH}$ (proton attacks N from the opposite side of adsorbed OH) system at 400 K within 10 ps AIMD simulation..

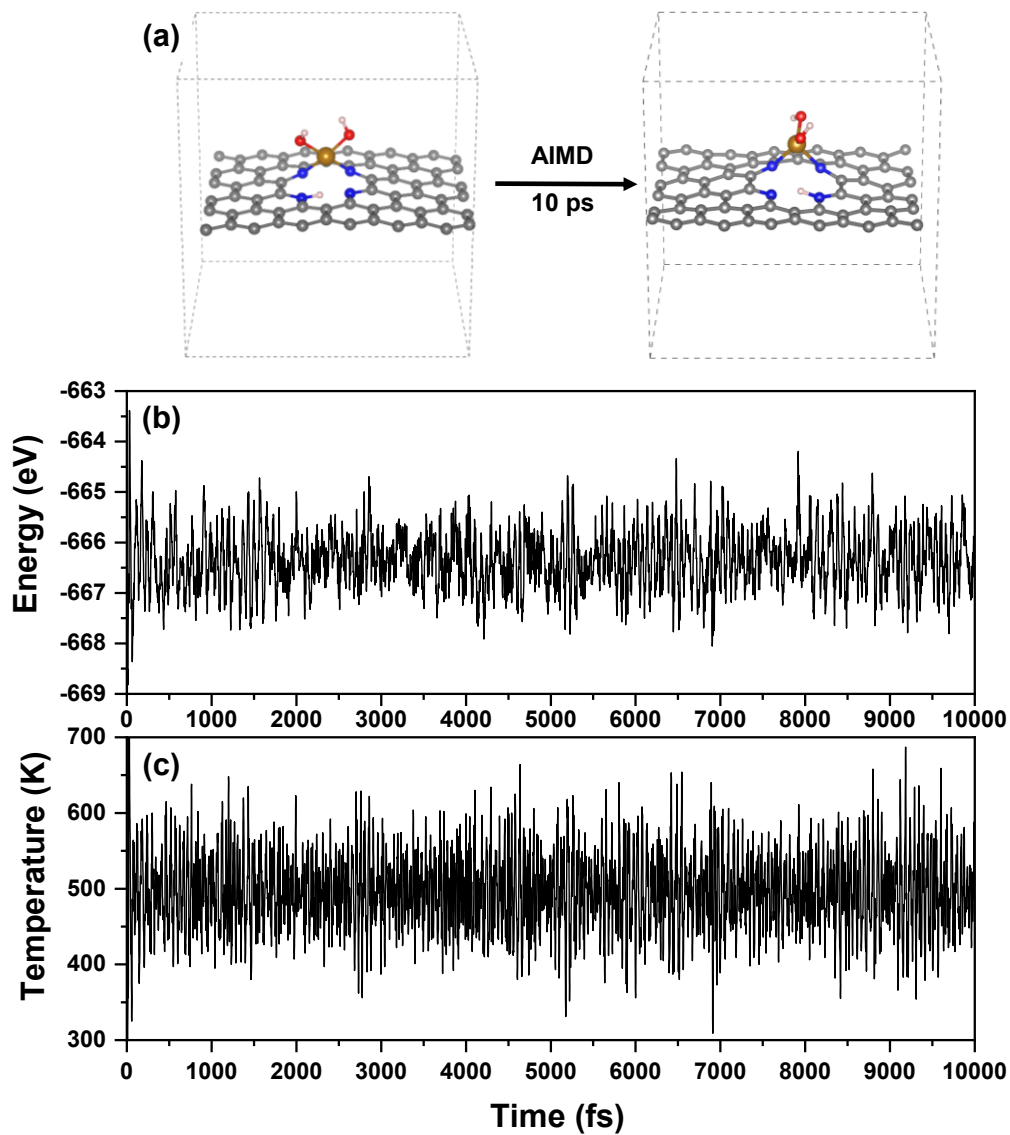


Figure S17. (a) Dynamic optimized configuration snapshot (b) total energy and (c) temperature of $*\text{Fe}(\text{OH})_2\text{-NH}$ (proton attacks N from the opposite side of adsorbed OH) system at 500 K within 10 ps AIMD simulation..

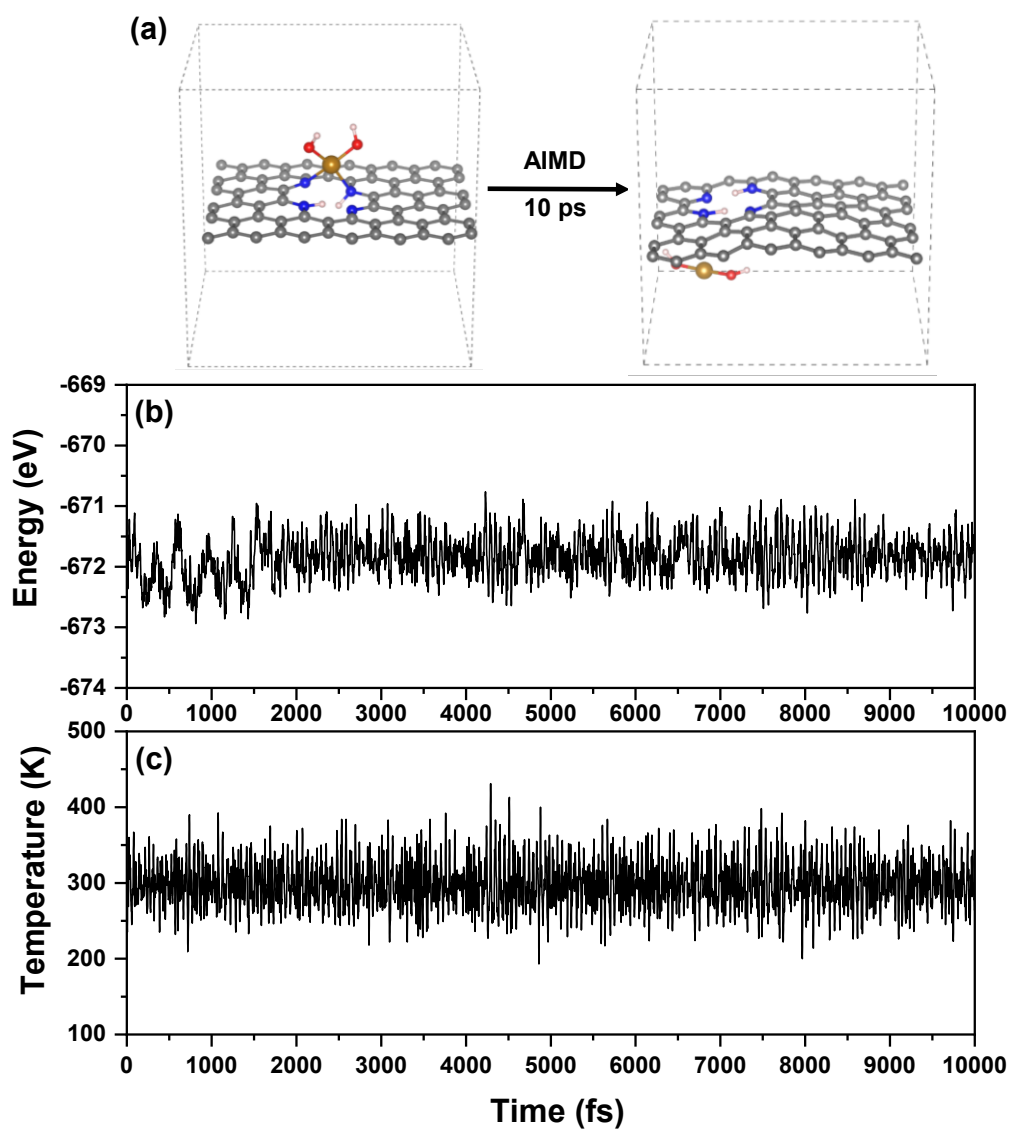


Figure S18. (a) Dynamic optimized configuration snapshot (b) total energy and (c) temperature of *Fe(OH)₂-NH + H system at 300 K within 10 ps AIMD simulation.

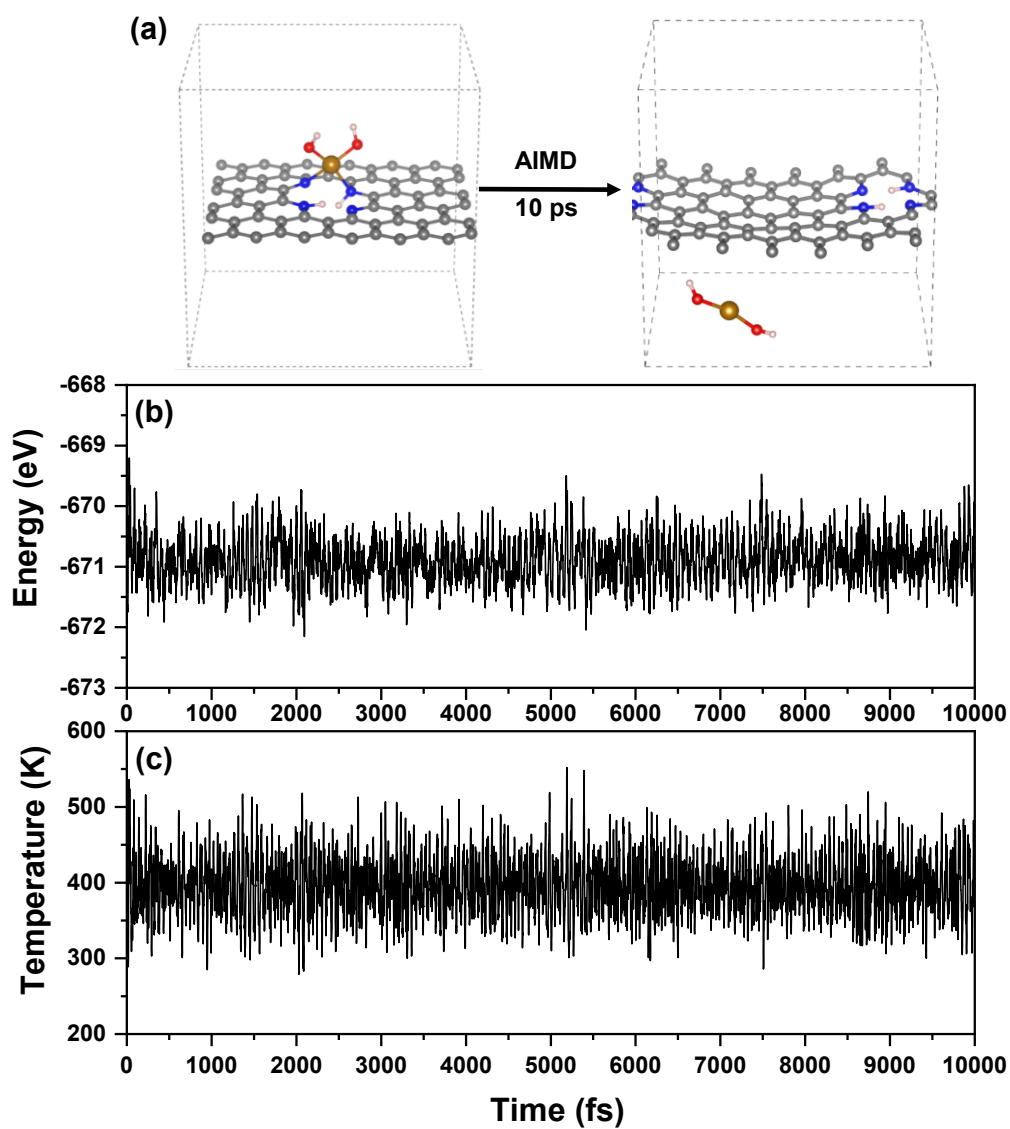


Figure S19. (a) Dynamic optimized configuration snapshot (b) total energy and (c) temperature of $^*Fe(OH)_2-NH + H$ system at 400 K within 10 ps AIMD simulation.

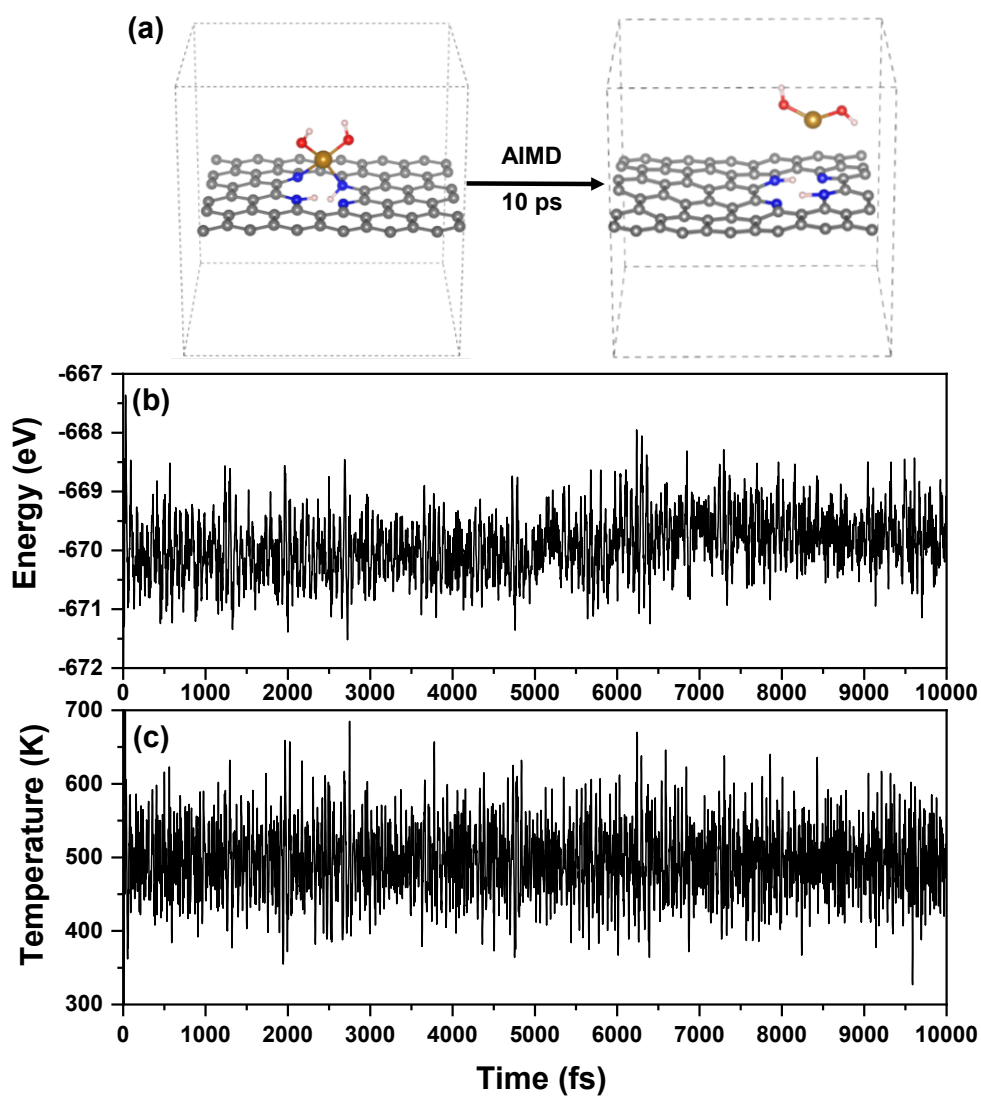


Figure S20. (a) Dynamic optimized configuration snapshot (b) total energy and (c) temperature of $*\text{Fe}(\text{OH})_2\text{-NH} + \text{H}$ system at 500 K within 10 ps AIMD simulation.

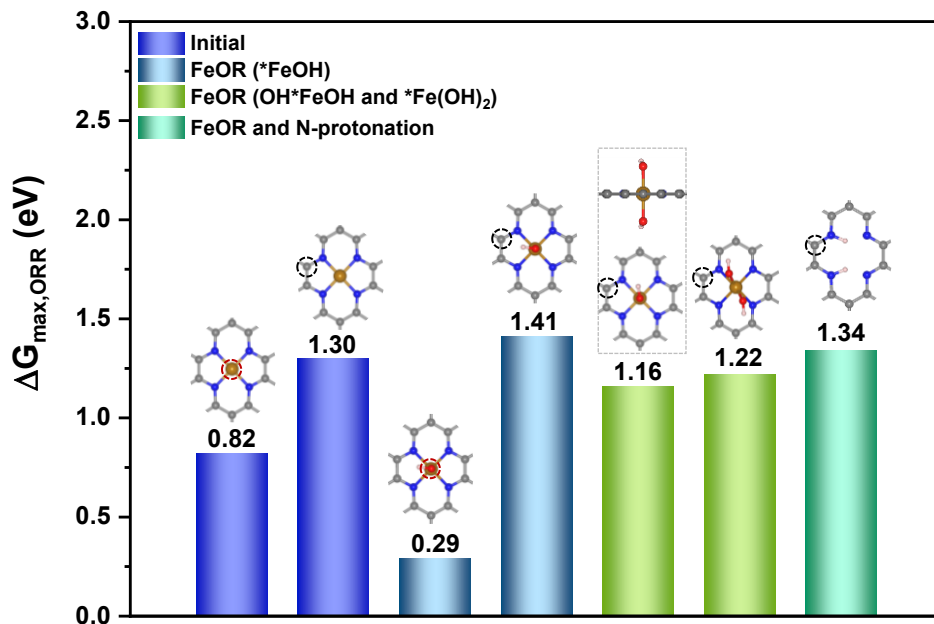


Figure S21. The $\Delta G_{\max, \text{ORR}}$ of the FeNC before and after oxidation of Fe site and protonation of N site, where the active site in dotted line.

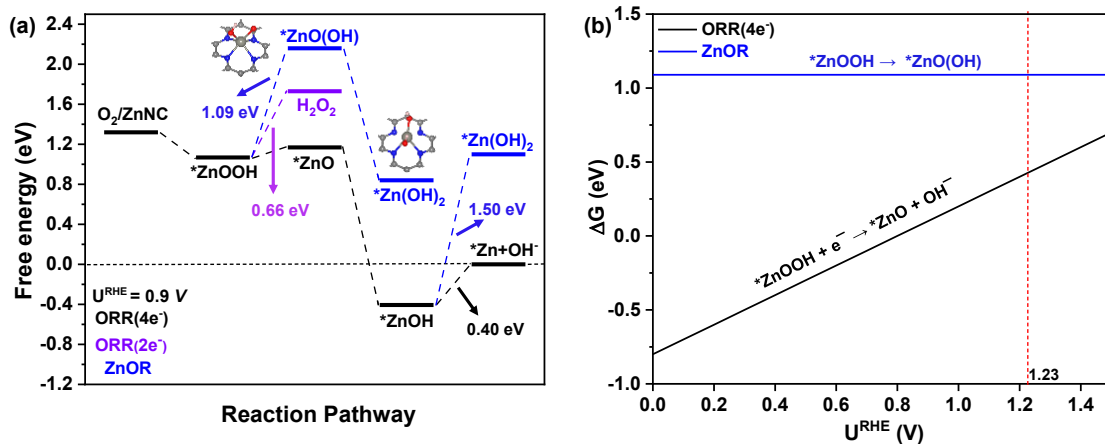


Figure S22. a) At $U^{\text{RHE}} = 0.9 \text{ V}$, the free energy diagram on Zn site of ZnNC catalyst surface, b) The ΔG value of ORR($4e^-$) and ZnOR as a function of U^{RHE} .

Video S1. The AIMD dynamic graph of the protonation and oxidation of Fe site on FeNC in real water solution.



(a) FeN4H-water.mp4



(b) Fe(OH)₂-water.mp4

Video S2. The AIMD dynamic graph of the protonation of *Fe(OH)₂.



(a) Fe(OH)₂-NH-same-side.mp4



(b) Fe(OH)₂-NH-opposite-side.mp4

Reference

(S1) CRC Handbook of Chemistry and Physics. 1219.

(S2) Skulason, E.; Bligaard, T.; Gudmundsdottir, S.; Studt, F.; Rossmeisl, J.; Abild-Pedersen, F.; Vegge, T.; Jonsson, H.; Norskov, J. K., A theoretical evaluation of possible transition metal electro-catalysts for N₂ reduction. *Phys. Chem. Chem. Phys.* **2012**, *14*, 1235-45.

(S3) Li, L.; Martirez, J. M. P.; Carter, E. A., Prediction of Highly Selective Electrocatalytic Nitrogen Reduction at Low Overpotential on a Mo-Doped g-GaN Monolayer. *Acs Catal.* **2020**, *10*, 12841-12857.